Modelling of Hybrid Scenario: from present-day experiments toward ITER

X. Litaudon[1], I. Voitsekhovitch[2], J.F. Artaud[1], P. Belo[3], J.P.S. Bizarro[3], T Casper[4], J. Citrin[5], E. Fable[6], J. Ferreira[3], J. Garcia[1], L. Garzotti[2], G. Giruzzi[1]J. Hobirk[6], G.M.D. Hogeweij[5], F. Imbeaux[1], E. Joffrin[1], F. Koechl[7], F. Liu[1], J. Lönnroth[8], D. Moreau[1], V. Parail[2], P.B. Snyder[9], M. Schneider[1], ASDEX Upgrade Team, JET-EFDA contributors[*], and the EU-ITM ITER Scenario Modelling group

[1]CEA, IRFM, F-13108 Saint Paul Lez Durance, France
[2]EURATOM/CCFE Fusion Association, Culham Science Centre, Abingdon OX14 3DB UK
[3]Associacão EURATOM-IST, Instituto de Plasmas e Fusão Nuclear, Lisbon, Portugal
[4]ITER Organization, F-13115 Saint Paul lez Durance, France
[5]FOM Institute DIFFER—Dutch Institute for Fundamental Energy Research, Association EURATOM-FOM, Nieuwegein, The Netherlands
[6]Max-Planck-Institut für Plasmaphysik, EURATOM-Assoziation, Garching, Germany
[7]Association EURATOM-ÖAW/ATI, Atominstitut, TU Wien, 1020 Vienna, Austria
[8]Helsinki University of Technology, Association EURATOM-Tekes, P.O.Box 4100, FIN-02015 TKK, Finland
[9]General Atomics, San Diego, USA

e-mail of first author: xavier.litaudon@cea.fr

Abstract. The 'hybrid' scenario is an attractive operating scenario for ITER since it combines long plasma duration with the reliability of the reference H-mode regime. We review the recent European modelling effort carried out within the ITER Scenario Modelling group which aims at (i) understanding the underlying physics of the hybrid regime in ASDEX-Upgrade and JET, and, (ii) extrapolating them toward ITER. JET and ASDEX-Upgrade hybrid scenarios performed under different experimental conditions have been simulated in an interpretative and predictive way in order to address the current profile dynamics and its link with core confinement, the relative importance of magnetic shear, *s*, and *ExB* flow shear on the core turbulence, pedestal stability and H-L transition. Projections to ITER hybrid scenarios have been carried out focusing on optimization of the heating/current drive schemes to reach and control the desired plasma equilibrium using ITER actuators.

1. Introduction

An attractive operating scenario for ITER has recently emerged that combines long plasma duration similar to the steady-state scenario, together with the reliability of the reference H-mode regime. The so-called 'hybrid' scenario aims to maximize neutron fluence with an extended burn time (t>1000s) together with significant fusion gain, Q>5 [1-2]. Worldwide a significant experimental effort has been devoted to explore the operating space in present day tokamaks. This paper is an overview of the recent European modelling effort carried out within the ITER Scenario Modelling working group, ISM-WG, which aims at (i) understanding the underlying physics of the hybrid regime in ASDEX-Upgrade and JET, and, (ii) extrapolating them toward ITER. The ISM-WG is organized within the EFDA Task Force on Integrated Tokamak Modelling (ITM-TF). The main responsibility of the ISM-WG is to advance a pan-European approach to (i) interpretative modelling of existing experiments to validate and benchmark integrated modelling tools and (ii) to predictive modelling of ITER plasmas with the emphasis on urgent issues. In this paper, plasma current density evolution, heat, particle and momentum transport, and pedestal characteristics in JET and ASDEX-Upgrade hybrid discharges are investigated by means of various integrated modelling tools (ASTRA, JETTO, CRONOS). Predictions of ITER hybrid scenarios are then carried out

[*] See the Appendix of F. Romanelli et al., Proceedings of the 24th IAEA Fusion Energy Conference 2012, San Diego, USA

making use of the findings obtained from the analysis of existing experiments. This paper complements (i) previous European studies performed within the ISM-WG focusing on the ITER baseline scenario [3], (ii) the international effort coordinated by the Steady State Operation (SSO) topical group of the International Tokamak Physics Activity (ITPA) to compare the various codes prediction for the Hybrid and steady-state scenarios [4] and (iii) finally the most recent ITER predictive modelling of three main scenarios performed within an F4E grant [5]. The paper is organized in two main sections. In section 2, recent integrated modelling of the JET and ASDEX-U hybrid scenario is discussed. In section 3, extrapolation of our validation exercise on existing experiments to ITER hybrid scenario is performed.

2. Integrated modeling of ASDEX-U and JET hybrid scenario

More than fourteen JET and two ASDEX-Upgrade hybrid scenarios performed under different experimental conditions (plasma shape, heating power, plasma current ramp-up waveform, dimensionless parameters etc.) have been simulated in an interpretative and predictive way in order to address the current profile dynamics and its link with confinement, the relative importance of magnetic shear, *s*, and *ExB* flow shear on the core turbulence, pedestal stability and H-L transition. For both machines, a variation in q-profile at the start of the main heating phase was experimentally achieved but using different techniques. By optimising the current density profile (i.e. broadening the current profile with flat core q profile over a large part of the plasma radius), enhanced confinement factor, $H_{IPB98(y,2)}$, with respect to the IPB98(y,2) scaling have been observed up to levels of 1.4. For JET, this variation was achieved via the 'current-overshoot' method [6, 7]. For ASDEX-Upgrade, the q-profile modification was achieved by varying the auxiliary heating timing, with the later heating case resulting in a broader q-profile [8].

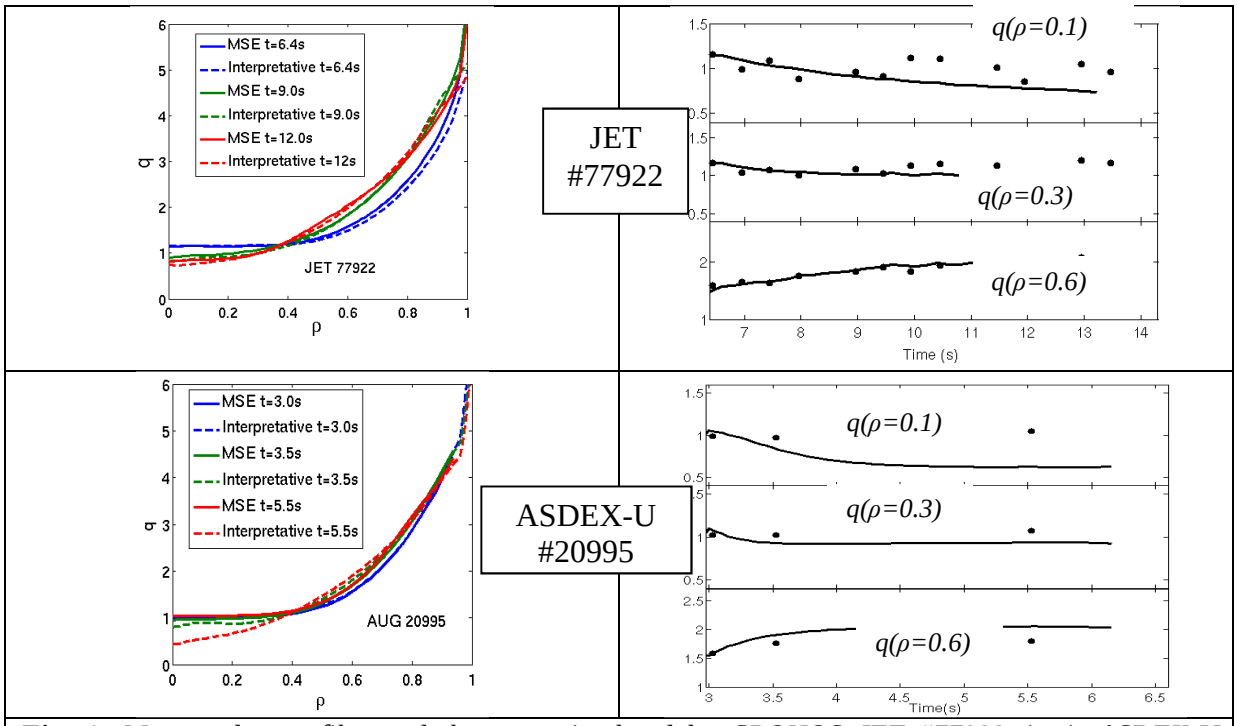

Fig. 1: *Measured q-profiles and the ones simulated by CRONOS JET #77922 (top), ASDEX-U #20995 (bottom). (left) radial profiles at different times; (right) time evolution: experimental data (full circles) and CRONOS simulation (solid line) at ρ=0.1, ρ=0.3 & ρ=0.6*

2.1 Current diffusion

Current diffusion using neo-classical prediction for the resistivity and bootstrap current is simulated for JET and ASDEX-U with the CRONOS code [9] by doing an interpretative analysis with the same modelling assumptions. The simulations are initiated at the time when the first MSE data are available (just after the NBI application). The initial magnetic equilibrium is prescribed by the first q-profile determined by the magnetic reconstruction constrained by MSE measurement. The simulated q-profiles with CRONOS using the measured kinetic profiles (temperature and density) are then compared at each time step to the other MSE measurements. In JET hybrid discharges and in the absence of MHD activity, the current profile slowly relaxes after the H-mode transition with on-axis q_o~1 and its dynamics is reasonably well reproduced with the neo-classical approximation as shown in Fig. 1 (similar results have been obtained for the 20s long hybrid discharge #77280, which last for 3 current diffusion times). Conversely, for ASDEX-U it is found that the q-profile is rapidly clamped to the q_o=1 surface in the studied discharge #20995 while neo-classical current diffusion simulation predicts a slow relaxation with q_o below unity.

2.2 q-profile influence on transport

Modelling effort is carried out to isolate the impact of increased *s/q* at outer radii (where *s* is the magnetic shear) on core confinement in low-triangularity JET and ASDEX-Upgrade experiments [10]. Predictive heat and particle transport is calculated using the integrated modelling code CRONOS coupled to the GLF23 turbulent transport model [11]. For both machines, discharge pairs were analysed displaying similar pedestal confinement yet significant differences in core confinement. For the JET pair (#79626 with $H_{IPB98(y,2)}$~1.3/#79630 with $H_{IPB98(y,2)}$~1.1), this variation was respectively achieved with or without the 'current-overshoot' method. For the AUG pair (#20993/#20995), the q-profile variation was achieved by varying the auxiliary heating timing, with the later heating case resulting in a broader q-profile with improved confinement (#20995, $H_{IPB98(y,2)}$~1.2) compared to the reference case (#20993, $H_{IPB98(y,2)}$~1.0). Both heat transport only simulations (with prescribed density profiles) and combined heat and particle transport simulations are carried out by including or not the *ExB* shear stabilisation effect [10]. For each discharge, comparison simulations were carried out substituting the q-profile input with the q-profile from the other member of each pair. In such a manner GLF23 predicts the confinement difference solely due to the q-profile. Fig. 2 display results of combined heat and particle transport from GLF23 simulation (without *ExB* shear stabilisation) comparing results with q-profile inputs taken from either the low or high confinement discharges. Correlation of the improved confinement with an increased *s/q* at outer radii, observed in low triangularity JET and ASDEX-Upgrade discharges, is consistent with the predictions based on the GLF23 model. This effect accounts for ~60-90% and ~35-55% of the core confinement improvement in JET and ASDEX-Upgrade respectively (Fig. 2). These results are consistent with an increase of the ITG threshold with *s/q*. When including the *ExB* suppression effect, (with $\alpha_E=\gamma_{max}/\gamma_E=1.35$, γ_{max} is maximum linear growth rate, γ_E is the *ExB* shear rate) GLF23 is found to overestimate the core thermal energy content by at least 40%.

2.3 Self-consistent modelling of hybrid scenario: *ExB* shear influence on transport

Self-consistent four-field simulations predicting the electron (T_e) and ion (T_i) temperatures, main ion density (n_i) and toroidal angular frequency (ω) have been performed for eight JET pulses [12] with GLF23 model in ASTRA [13]. Four low δ and three high δ hybrid discharges

are analysed with different parameters and $H_{IPB98(y,2)}$ from 1 to 1.37. The NBI heat, particle and momentum sources have been calculated with NUBEAM/TRANSP, while the deuterium neutral influx has been estimated in the self-consistent TRANSP-EDGE2D simulations. The GLF23 model applied with α_E=1, gives a satisfactory prediction for JET H-mode plasmas [14], but under-predicts in hybrid regime n_i and ω (Fig. 3, left). With α_E=0.5 a more accurate n_i, ω and T prediction has been achieved. These simulations have been repeated assuming that the momentum diffusivity χ_φ is a fraction of the thermal ion diffusivity χ_I (Fig. 3 right). With P_r=0.3 and 0.5 for respectively low and high δ pulses an improvement in the prediction of ω has been achieved while n_i and T remains within 20% deviation from the measurements.

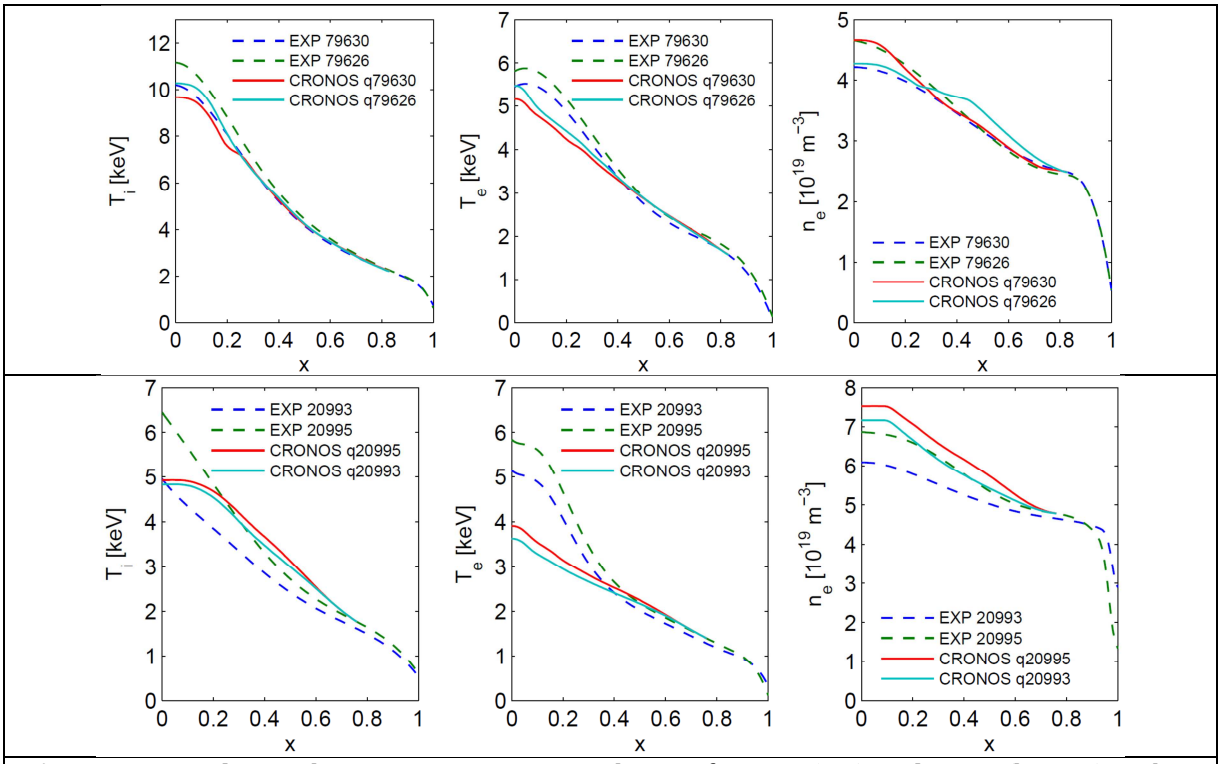

Fig. 2: *Heat and particle transport GLF23 simulations for JET (top) and AUG (bottom) without ExB stabilisation effect. (left column) T_i profiles. (center column) T_e profiles. (right column), n_e profiles. (top): JET 79630, comparing q-profile inputs from both 79630 and 79626. (bottom) AUG 20995, comparing q-profile inputs from both 20995 and 20993. [from 10]*

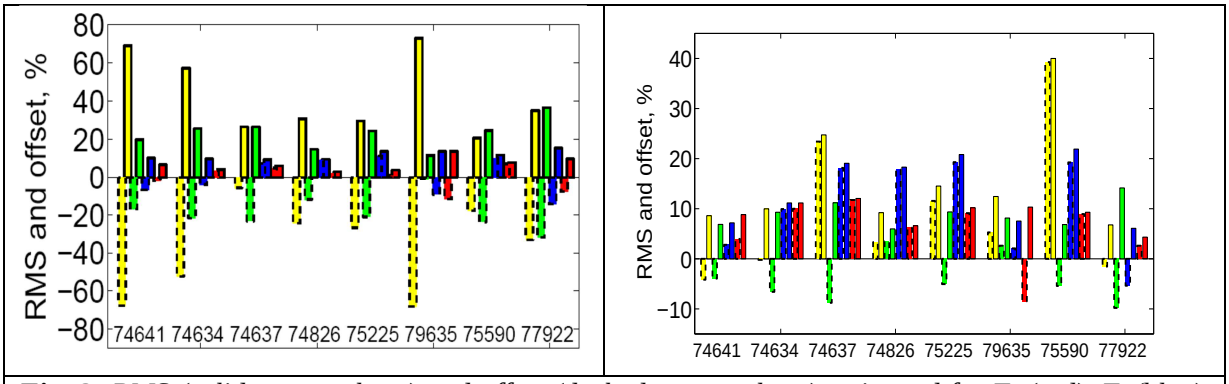

Fig. 3*: RMS (solid contour bars) and offset (dashed contour bars) estimated for T_e (red), T_i (blue), n_D (green) and ω (yellow) using (left) α_E=1 and GLF23 computed χ_φ and (right) α_E=0.5, χ_φ=Pr·χ_i with Pr=0.3 (low δ) and 0.5 (high δ) discharges. H-mode pulse 74826 has been simulated using α_E=1. [from 12]*

3. Predictive integrated modeling of ITER hybrid scenario

A set of simulations of the ITER hybrid scenario is performed with the 0.5-D code METIS [15] which is a module included in CRONOS. The main advantage of METIS consists in providing fast calculation in order to scan the operational domain and to define the domain where ITER hybrid scenario could exist while imposing the double constrain of having $q_0>1$ for long duration (1000s) and the ratio of fusion to additional powers, Q_{DT}, $Q_{DT}>5$. ITER hybrid scenarios have been calculated at a plasma current $Ip=12MA$ at $B_T=5.3T$ ($q_{95}=4.3$), with the ITER baseline heating mix 20MW ICRH, 33MW NBI, 20MW ECCD and with a line averaged density fixed to $n_l=7.5x10m^{-3}$ ($n_l/n_{Gw}\sim0.8$) during the burn phase. The parameters that have been scanned are the density peaking factor with $n_{eo}/n_l=1,1.2,1.4$ and $H_{98IPB(y,2)}\sim1.1, 1.2, 1.25, 1.3, 1.4$ with the corresponding pedestal pressure of *87kPa, 90kPa, 92kPa, 95kPa, 100kPa*. Fig. 4 (left) shows the time evolution of the plasma scenario (assuming $H_{98IPB(y,2)}\sim1.4$) with three different values of n_{eo}/n_l keeping the same line averaged density (i.e. an increase of n_{eo}/n_l is obtained by increasing the core density while reducing the pedestal one). With the assumed baseline heating mix and the neo-classical current diffusion, METIS calculations indicate that high confinement and peaked density profiles are required to increase the bootstrap current at level above a certain value ($I_{boot}\sim4MA$ or $I_{boot}/I_p\sim30\%$ for the case shown on Fig. 4) to sustain the q-profiles above unity. Fig. 4 (right) presents the results of the full sensitivity studies where the I_{boot}/I_p and Q_{DT}, have been plotted versus $H_{98IPB(y,2)}$ for the three density peaking. It confirms that the operational domain with $q_0>1$ for more than 1000s and Q_{DT} > 5 is relatively narrow and requires high confinement and peaked density profile.

3.1 Current profile optimization during current ramp-up phase

Access condition to the class of hybrid-like q-profiles during the prelude phase of the scenario is investigated with particular attention in [16]. Validation on the ramp-up phase of JET, AUG and Tore Supra [17, 18] has shown that both empirical scaling based models and the semi-empirical Bohm/gyro-Bohm model yield a good reproduction of this phase. These models have been used in the optimisation of the current ramp-up phase carried out with CRONOS. Current ramp-up scenario is systematically investigated in view of (i) optimising the q-profile at the start of the current plateau for improved fusion performance, and, (ii) minimizing the resistive flux consumption to allow for long pulse operation while keeping the current in the central solenoid and poloidal field coils within the ITER operational limits. The optimisation of the q-profile relies on reaching a target q-profile that improves stability and energy confinement. It is concluded that minimising the resistive flux consumption and optimizing the q profile might be conflicting requirements. A trade-off between these two requirements has to be made. It is shown in [15,16] that fast current ramp with current overshoot is at the one extreme, i.e. optimum q profile at the cost of increased resistive flux consumption, whereas early H-mode transition is at the other extreme. It is found that the ITER heating systems allow reaching a hybrid q-profile at the end of the current ramp-up.

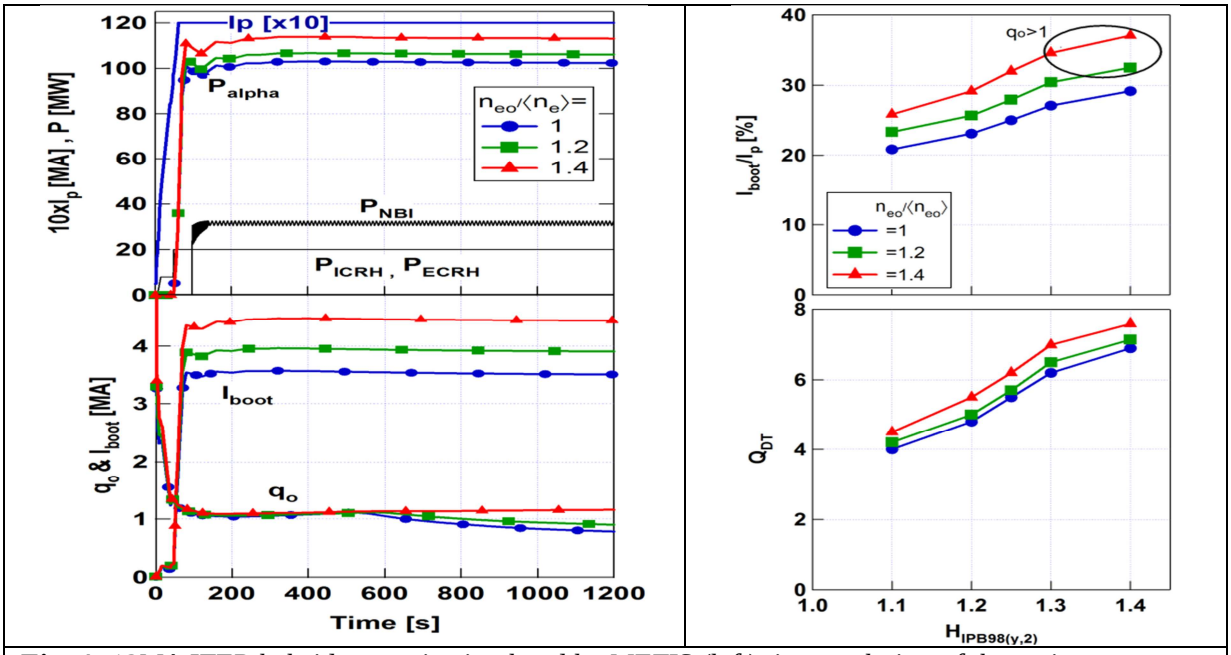

Fig. 4: *12MA ITER hybrid scenario simulated by METIS (left) time evolution of the main parameters assuming $H_{98IPB(y,2)}$=1.4 with three n_{eo}/n_l . (right) I_{boot}/I_p and Q_{DT} versus $H_{98IPB(y,2)}$ for three n_{eo}/n_l*

3.2 Core and pedestal integrated modeling with first principle predictive model

Accurate prediction of the edge transport barriers is essential to assess and optimise ITER fusion performance. In this context, the EPED pedestal model [19] has been applied to ITER hybrid scenarios. EPED is a first-principle model for predicting the H-mode pedestal height and width based upon two fundamental and calculable constraints: (1) onset of non-local peeling–ballooning modes at low to intermediate mode number, (2) onset of nearly local kinetic ballooning modes at high mode number. Calculation of these two constraints allows a unique, predictive determination of both pedestal height and width without any free or fitting parameters. The EPED model has been extensively tested across a range of experiments on several devices [19]. The EPED pedestal model has been applied to ITER hybrid scenarios. The inputs to the model are: $B_t(T)$, $I_p(MA)$, $R(m)$, $a(m)$, δ, κ, $n_{e,ped}$ ($10^{19}m^{-3}$), Z_{eff}, β_N, where $n_{e,ped}$ is the pedestal electron density. For the ITER hybrid simulation the following equilibrium parameters were set to R=6.2m, a=2m, κ=1.85, δ=0.485, B_t=5.3T. Predictions for the hybrid scenario have been made for the pedestal height and width at various plasma currents (I_p=11, 12, 13MA), effective charge (Z_{eff}=1.7, 2.5), pedestal density ($n_{e,ped}$=6.5, 7.5, 8.5, 9.5, 10.5x10^{+19}m^{-3}) and β_N =1.8, 2.2, 2.6, 3.0. For this density range, it was found that the β_N dependence is weak and the results shown on Fig. 5 (left) have been obtained for β_N=2.2. The results of the I_p-scan are shown on Fig. 5 (left) where the pedestal heights are plotted versus the pedestal width for various densities and for two Z_{eff} values. Fig. 5 (left) shows that by increasing Z_{eff} from 1.7 to 2.5 increases the predicted pedestal pressure. Similarly, EPED model predicts that the pedestal height increases with density (collisionality dependence of the kink/peeling stability limit).

Hybrid scenario performance in ITER is studied with the CRONOS integrated modelling suite, using the GLF23 anomalous transport model for heat transport prediction and by imposing the values for the pedestal width and height as calculated separately by EPED. From the interpreted role of the *s/q* ratio in experiments, ITER hybrid scenario has been optimized through tailoring the q-profile for various assumed pedestal conditions. We investigate the importance of the density peaking on the fusion performance and q-profiles using

simultaneously first principle models for the core heat transport and pedestal width. The scenario is an extension to the one published in [20] with the pedestal parameters obtained from EPED. ITER hybrid scenarios were calculated at a plasma currents *Ip=11.5-11.8MA* at B_T*=5.3T* with the ITER baseline heating mix 33MW NBI, 20MW ECRH, 20MW ICRH (53 MHz, 2nd T harmonic), and with $n_l=8.8x10^{19}m^{-3}$ (n_l/n_{Gw}*~0.95*). The main CRONOS assumptions are as follows: equal ratios of D and T are assumed, q-profile evolution is predicted by modelling the current diffusion with the neoclassical resistivity calculated by the NCLASS model, electron and ion heat transport are predicted, the density profile is prescribed. Rotation is set to zero and GLF23 is applied with α-stabilization off. GLF23 calculates the anomalous transport in the core for the bulk of the volume inside the pedestal top, between ρ*=0.25-0.92*. Three different values of n_{eo}/n_l*=1,1.25,1.5* have been selected while keeping the same line averaged density. The temperature pedestal tops are set at ρ*=0.92* in accordance with the EPED predicted height and widths. In our simulations, this location sets the boundary values for the GLF23 predictions. The kinetic and q-profiles produced at the end of the burn phase (1200s) are shown on Fig. 5 (right). When imposing first principle calculation for the core and pedestal transport and with the ITER baseline heating & current drive mix, the calculation indicates that: (i) the thermal enhanced confinement factor, $H_{IPB98(y,2)}$ is around unity, (ii) the resulting bootstrap current fraction is around 30% (β_N ~2) which is the marginal value to maintain the q-profile above unity, (iii) the increase of the n_{eo}/n_l at fixed density weakly affects the fusion performance and the ability to sustain q_0 above unity for more than 1000s. Indeed, when increasing the density peaking, the density at the pedestal top is reduced which leads (EPED prediction) to a reduction of the pressure at the pedestal top.

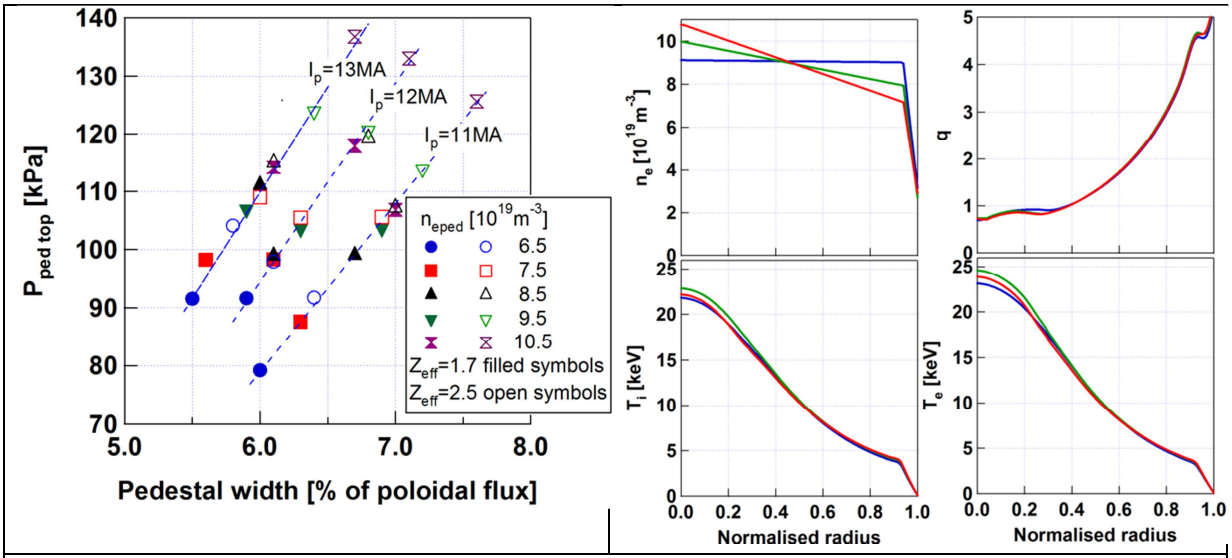

Fig. 5: *(left) EPED prediction for ITER hybrid scenario; Pressure at the top of pedestal versus pedestal width for different pedestal densities, n_{eped}, Z_{eff} and I_p. (right) CRONOS ITER hybrid scenario predictive modeling with EPED constrains; T_e, T_i and q profiles (at 1200s) with three different imposed density profiles.*

3.3 Model-based Magnetic and Kinetic real time Control

In hybrid or steady state scenarios, simultaneous magnetic and kinetic control of plasma profiles and parameters such as the current profile, the pressure profile, and the alpha-particle power are essential to maintain high performance for durations that exceed the resistive diffusion time. An integrated model-based plasma control strategy, ARTAEMIS, has been initiated on JET and pursued on JT-60U and DIII-D, and closed-loop control of the poloidal

flux, safety factor and β_N has been recently performed in DIII-D [21, 22]. The general model-based approach has also been applied to the ITER hybrid regime for the control of the magnetic equilibrium (poloidal flux profile) and of the alpha-particle power, P_α [22, 23]. The control actuators are the two ITER neutral beam injectors, the ECRH, ICRH and lower hybrid (LHCD) systems, and the plasma surface loop voltage. The nonlinear plasma response to the actuators is modeled with METIS. A two-time-scale model was identified from a set of open-loop simulations using the ARTAEMIS algorithm. Closed-loop control simulations were performed by inserting the METIS code at the output of the two-time-scale ARTAEMIS controller. In these simulations, various target profiles for the poloidal flux have been obtained simultaneously with various target levels of fusion power [22, 23]. This shows that current profile control can be combined with burn control, sharing a common set of actuators.

Acknowledgement This work, supported by the European Communities under the contracts of Association between EURATOM and CEA, CCFE, IST, FOM, IPP, ÖAW, TEKES was carried out within the framework of the Task Force on Integrated Tokamak Modelling of the European Fusion Development Agreement. The views and opinions expressed herein do not necessarily reflect those of the European Commission.

References

[1] Gormezano C. et al 2007 Nucl. Fusion 47 S285
[2] Joffrin E. Plasma Phys. Control. Fusion 49 (2007) B629–B649
[3] Parail V. et al, Nucl. Fusion **49** (2009) 075030
[4] Kessel C.E. et al Nucl. Fusion **47** (2007) 1274–1284
[5] Parail V. et al this conference (2012)
[6] Joffrin E et al 2010 Proc. 23rd Int. Conf. on Fusion Energy 2010 (Daejeon, South Korea 2010) (Vienna: IAEA)
[7] Hobirk J et al Plasma Phys. Control. Fusion **54** (2012) 095001
[8] Stober J et al Nucl. Fusion **47** (2007) 728
[9] Artaud J.F. et al, Nucl. Fusion **50** (2010) 043001
[10] Citrin J. et al, Plasma Phys. Contr. Fusion **54** (2012) 065008
[11] Waltz R.E. et al 1997 Phys. Plasmas 7 2482
[12] Voitsekhovitch I. et al., in Proc. 39th EPS Conf on Plasma Physics and 16th International Congress on Plasma Physics (Stockholm, Sweden, 2012), Vol. **36F** file P4.066 (2012)
[13] Pereverzev G.V., Yushmanov P.N. 2002 Report IPP 5/98, Max-Planck-Institute fur Plasmaphysik
[14] Voitsekhovitch et al, Nucl. Fusion **49** (2009) 055026
[15] Artaud J.F. et al, in proceeding 32nd EPS Conf. on Plasma Phys. and Contr. Fusion, (Spain, Tarragona, 2005) ECA Vol. **29C**, P1.035 (2005)
[16] Hogeweij G.M.D. et al, Plasma & Fus Res. **7** (2012) 2403063 and sub to Nuc. Fusion
[17] Imbeaux F. et al, Nucl. Fusion **51** (2011) 083026
[18] Voitsekhovitch I. et al Plasma Phys. Contr. Fusion 52 (2010) 105011
[19] Snyder P.B. et al Nucl. Fusion **51** (2011) 103016 and Phys. Plasmas **19** (2012) 056115
[20] Citrin J. et al, Nucl. Fusion **50** (2010) 115007
[21] Moreau D. et al., Nucl. Fusion **48** (2008) 106001 and Nucl. Fusion **51** (2011) 063009
[22] Moreau D. et al., 2012, 24th IAEA Fusion Energy Conference, paper ITR/P1-20
[23] Liu F. et al., in Proc. 39th EPS Conference on Plasma Physics and 16th International Congress on Plasma Physics (Stockholm, Sweden, 2012), Vol. **36F** file P1.063 (2012)